Bioorganic & Medicinal Chemistry Letters 18 (2008) 3819–3843

Contents lists available at ScienceDirect

Bioorganic & Medicinal Chemistry Letters

journal homepage: www.elsevier.com/locate/bmcl

# Bioorganic & Medicinal Chemistry Letters Vol. 18, No. 14, 2008

## Contents

### ARTICLES

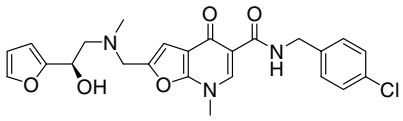

A new series of broad-spectrum herpesvirus polymerase inhibitors has been identified with antiviral activity against HCMV, HSV-1, EBV, and VZV. A practical synthesis of furo[2,3-*b*]pyridin-4-one-5-carboxylate esters is described.



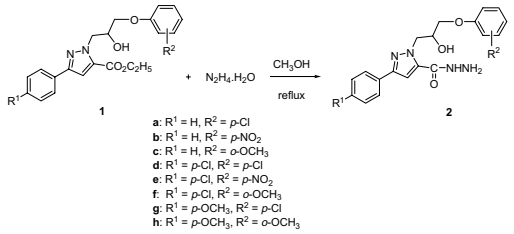


A series of novel 1-(2′-hydroxy-3′-aroxypropyl)-3-aryl-1*H*-pyrazole-5-carbohydrazide derivatives were synthesized. All of the 1-(2′-hydroxy-3′-aroxypropyl)-3-aryl-1*H*-pyrazole-5-carbohydrazide derivatives **2** could inhibit the growth of A549 cells in dosage- and time-dependent manners. Typically, compounds **2a** and **2d** induced A549 and H460 cells to autophagy, but did not inhibit the growth of HUVEC cells.



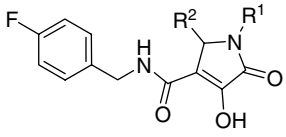

A series of novel 4-hydroxy-5-pyrrolinone-3-carboxamide HIV-1 integrase inhibitors was identified. SAR around the pyrrolinone core resulted in the discovery of compounds with inhibitory activity in the low nanomolar range.



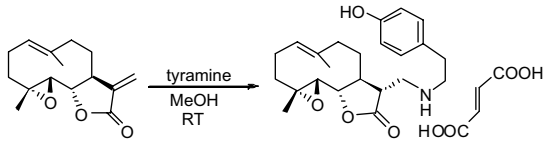


A series of aminoparthenolide analogs have been synthesized. Compound **12**, derived from tyramine, was found to be cytotoxic to acute lymphoblastic leukemia (ALL, CCRF-CEM) cells in culture at concentrations below 10 nM.

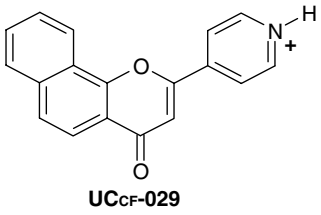


**$UC_{CF}$-029**

The effects of UCCF-029 on CFTR are compared with genistein.



Cyclobranol **8A**, an analog of the cycloartenol substrate **1A** for the plant sterol C24-methyltransferase (SMT), was shown to be an acceptor of the soybean SMT1 as well as an inhibitor of enzyme action. The $K_m$ and $k_{cat}$ for **8A** was 37 μM and 0.006 $min^{-1}$, respectively. The enzyme-generated product was identified by MS and $^1H$ NMR to be a C24, C25-doubly alkylated $\Delta^{24(28)}$-olefin **10A**. Inhibitor treatment was concentration and time-dependent affording an apparent $K_i$ of 25 μM, a maximum rate of inactivation of 0.15 $min^{-1}$ and a partition ratio ($k_{cat}/k_{inact}$) calculated to be 0.04.

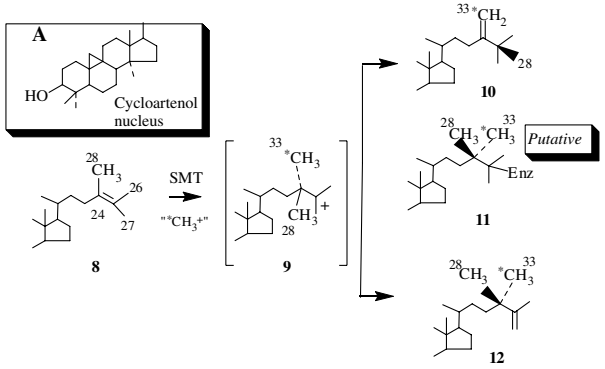




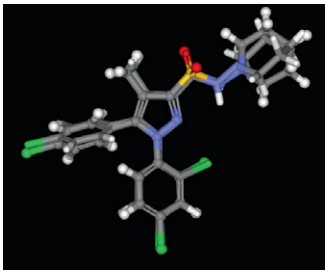

Facile synthesis of biaryl pyrazole sulfonamide derivative of 5-(4-chlorophenyl)-1-(2,4-dichlorophenyl)-4-methyl-1*H*-pyrazole-3-carboxylic acid piperidin-1-ylamide (SR141716, **1**) and an investigation of the effect of replacement of the –CO group in the compound **1** by the $–SO_2$ group in the aminopiperidine region is reported. Primary ex-vivo pharmacological testing of sulfonamide derivative **2** showed the loss of CB1 receptor antagonism.



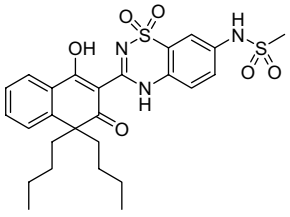


4,4-Dialkyl-1-hydroxy-3-oxo-3.4-dihydronaphthalene-3-yl benzothiadiazine derivatives were synthesized and evaluated as inhibitors of genotypes 1a and 1b HCV NS5B polymerase. A number of these compounds exhibited potent activity against genotypes 1a and 1b HCV polymerase in both enzymatic and cell culture activities. The representative compound above also showed favorable pharmacokinetics in the rat.

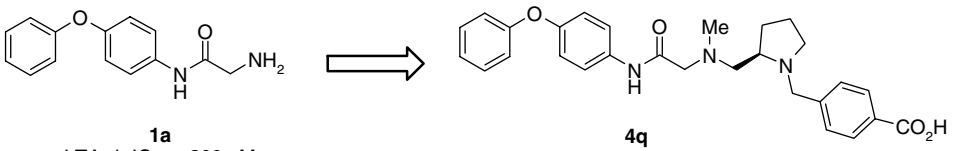




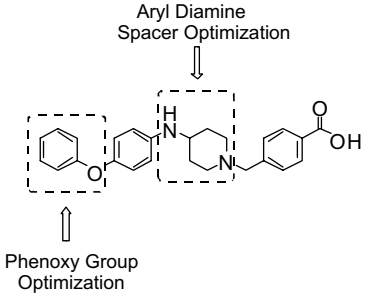




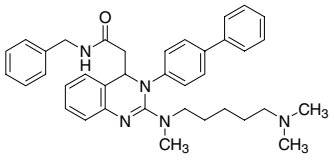




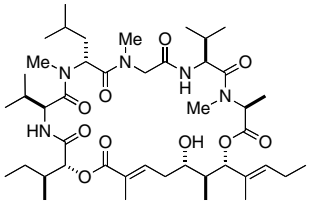


The artificial analogs of aurilide (**1**), a potent cytotoxic cyclodepsipeptide of marine origin, were synthesized, and the structure–activity relationships were investigated.

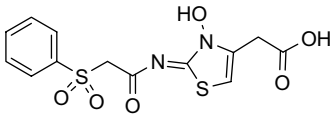


**1**

PHD2 $IC_{50}$ = 0.072 μM



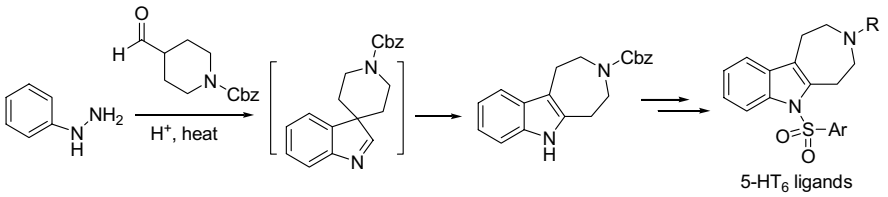


5-$HT_6$ ligands



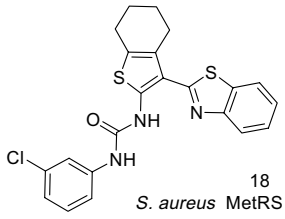


18

*S. aureus* MetRS $IC_{50}$ 6.3 μM

Multiple inhibitors of the antibacterial target, *Staphylococcus aureus* MetRS, were identified by virtual screening. The process consisted of building a Catalyst® pharmacophore from a ligand-*S. aureus* MetRS structure and using this pharmacophore to screen a commercial database. The top hits from this search were then docked into the *S. aureus* MetRS structure and this information was used to select compounds for testing. This resulted in a high hit rate of compounds that are in distinct structural classes from the known MetRS inhibitors.



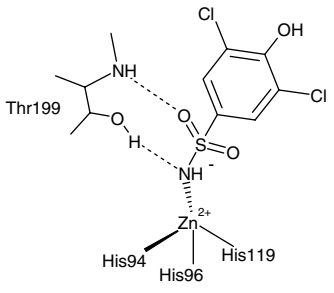

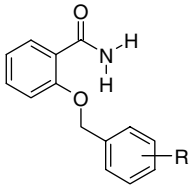

A novel series of alkoxybenzamides have been developed with restricted conformation through intramolecular hydrogen bond formation. The compounds exhibit low nM enzyme and cellular activity as poly(ADP-ribose) polymerase-1 (PARP-1) inhibitors.



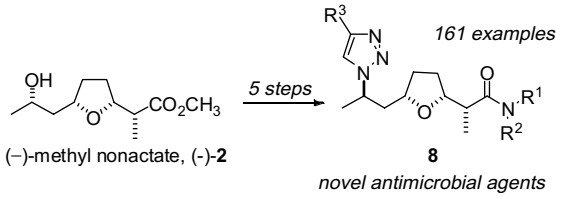




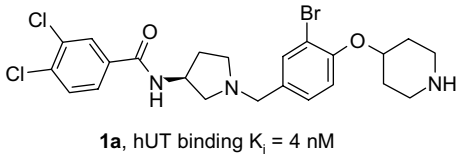


SAR exploration of the central diamine, benzyl, and terminal aminoalkoxy regions of the N-cyclic azaalkyl benzamide series led to the identification of very potent human urotensin-II receptor antagonists such as 1a with a $K_i$ of 4 nM. The synthesis and structure–activity relationships (SAR) of N-cyclic azaalkyl benzamides are described.



We discovered a novel series of potent and orally bioavailable PARP inhibitors containing a quaternary methylene-amino substituent at the C-2 position of the benzimidazole scaffold. Two optimized analogs, **9b** and **9k**, displayed excellent intrinsic and cellular potency, adequate pharmaceutical properties, and potentiated the efficacy of cytotoxic agent temozolomide (TMZ) in a B16F10 flank melanoma model.

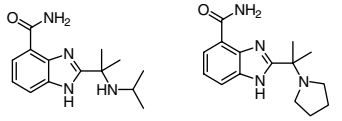

**9b** PARP-1 Ki= 7 nM
Cell $EC_{50}$= 2 nM
Mouse %F= 82

**9k** PARP-1 Ki= 3 nM
Cell $EC_{50}$= 0.9 nM
Mouse %F= 85

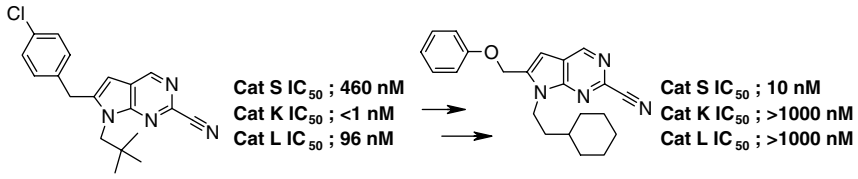




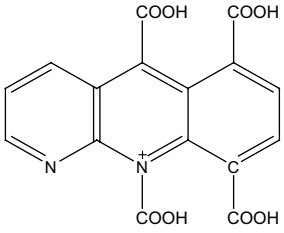


Quaternary Alkaloid



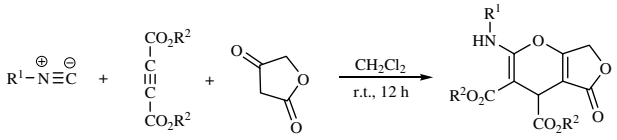




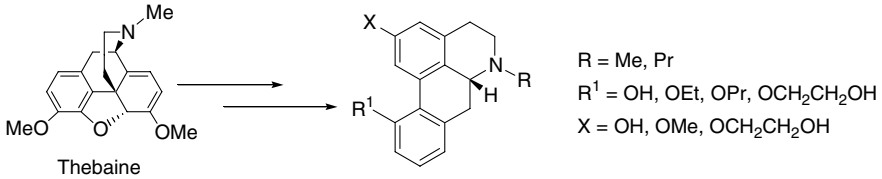


Thebaine

We synthesized several novel 2-*O*- or 11-*O*-substituted *N*-alkylnoraporphines and assessed their binding affinities at $D_1$, $D_2$ and 5-$HT_{1A}$ receptors in rat forebrain tissue. The most $D_2$-potent ($K_i$ = 97 nM) and selective novel agent (>100-fold vs. $D_1$ and 5-$HT_{1A}$ sites) was *R*(−)-2-(2-hydroxyethoxy)-11-hydroxy-*N*-*n*-propylnoraporphine (compound **11**).

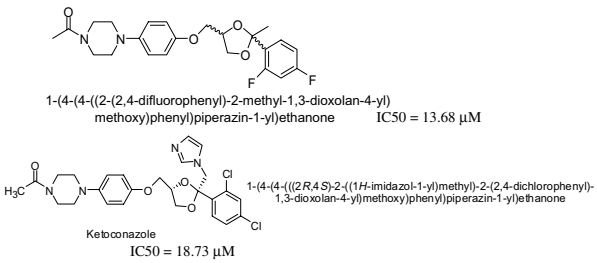




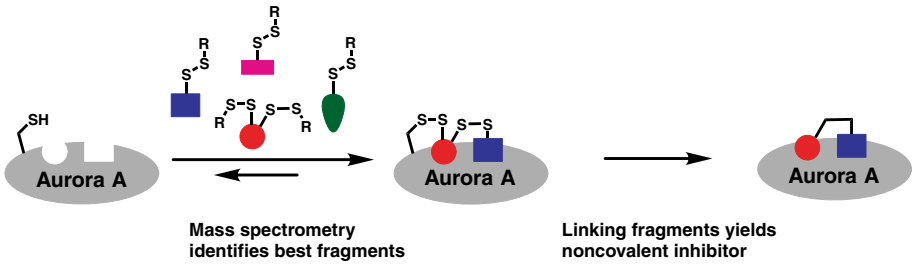


We demonstrate a fragment-based lead discovery method that combines site-directed ligand discovery with dynamic combinatorial chemistry to identify inhibitors of Aurora kinase A.



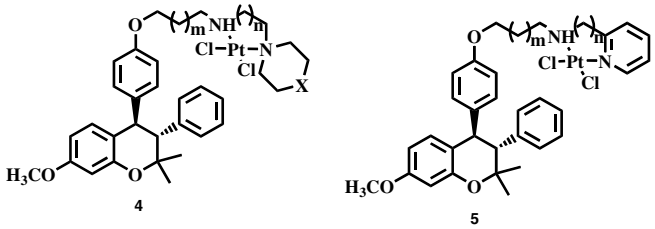


A series of benzopyran-based platinum complexes was synthesized as potential anticancer agents. The compounds were evaluated for their biological activity and showed significant in vitro cytotoxic activity in different breast cancer cell lines (MCF-7, MDA-MB-231, MDA-MB-436 and MDA-MB-468). Molecular modeling studies was performed to rationalize the results.



A novel cathepsin K inhibitor, [1-(2-cyano-tetrahydro-pyridazine-1-carbonyl)-2-methy-propyl]-carbamic acid benzyl ester (**8**, $IC_{50}$ = 1 nM), inhibited the bone resorptive activity of mature osteoclasts.

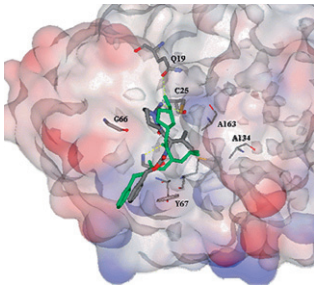

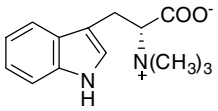


hypaphorine (**1**)

An indole alkaloid, hypaphorine (**1**) was isolated as a sleep inducing compound from the Brazilian medicinal plant, *Erythrina velutina* (Leguminosae). This compound was investigated for sleep promoting effects in mice, and significantly increased non-rapid eye movement (NREM) sleep time in mice during the first hour after its administration.



An optimized cDNA phage display cloning procedure is reported to simultaneously isolate two protein targets of cyclosporine A dependent on the binding affinity rather than the relative abundance in cells.

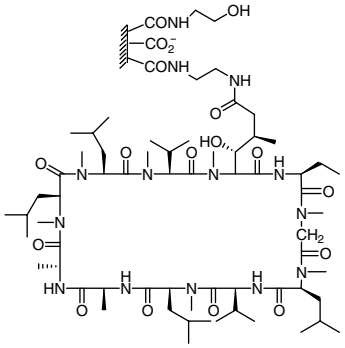


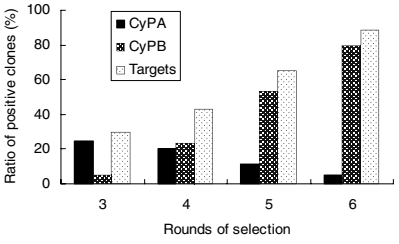




Peptide **1**: Ac-U-N-I-I-U-P-L-L-U-P-I-C* (Ac:acetyl; U: α-aminoisobutyric acid)
Peptide **2**: Ac-A-N-I-I-A-P-L-L-A-P-I-C*

Aib (α-aminoisobutyric acid)-containing peptide **1** can translocate into cells and the replacement of Aib with Ala (**2**) inhibits the cellular uptake. The translocation of the Aib-containing peptide seems to involve an energy-independent process.



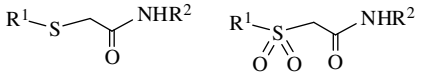


$R^1$ = mono-, disaccharides; $R^2$ = H, $C_8H_{17}$, $C_{12}H_{25}$

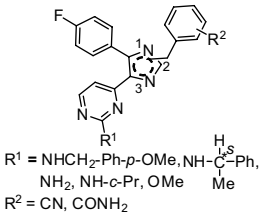




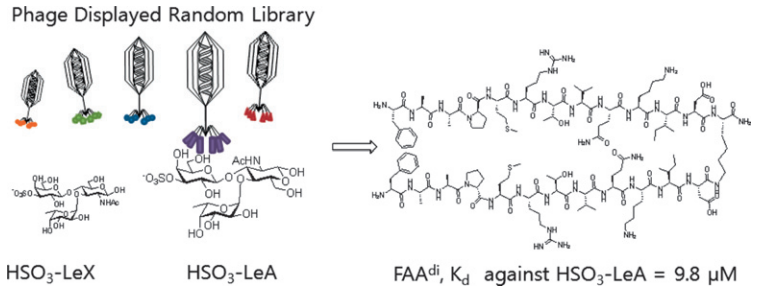




Phytochemical investigation of the roots of the *Saussurea lappa* yielded the new compound (**1**) along with known compounds (**2**–**5**). Anticancer active isolates and its derivatives were studied.

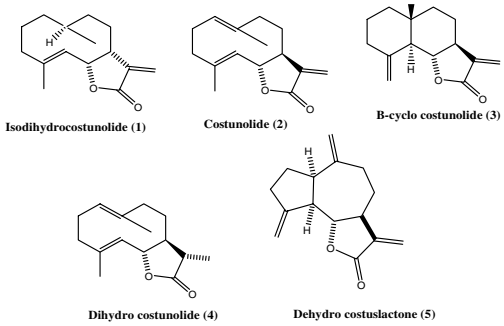




A series of substituted benzylamines **2**–**48** were prepared as part of a strategy to identify structurally differentiated and synthetically more accessible selective serotonin reuptake inhibitors, relative to clinical candidate **1**. In particular, **44** and **48**; demonstrated low nanomolar potency and good selectivity, in a structurally simplified template and, in vivo, very low Vdu, significantly lower than **I**, and a more rapid $T_{max}$, consistent with our clinical objectives.

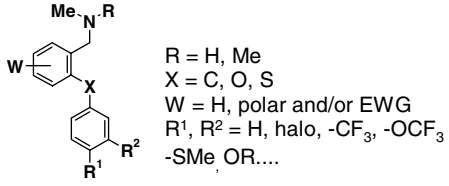


**2-48**

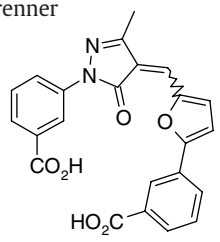

**1a**

WaaC is a new Gram-negative antivirulence target. The identification by virtual screening of the first micromolar inhibitor **1a** of this enzyme and the preliminary SAR generated from this family of aryl-pyrazolones is described.



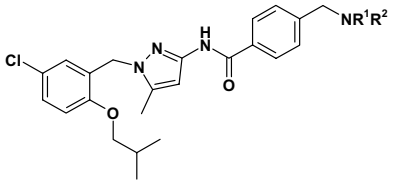

**4h: $NR^1R^2$ = NHEt**

**4j: $NR^1R^2$ = pyrrolidine**

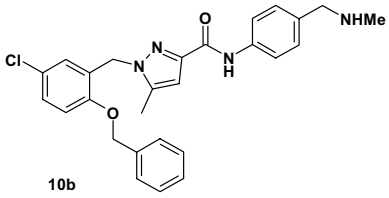

**10b**

This letter details the discovery and characterisation of a series of amides and reversed amides as $EP_1$ antagonists. Compounds such as **4h**, **4j** and **10b** displayed good solubility, CNS penetration and in vivo pharmacokinetic parameters but failed to show satisfactory oral exposure.



The synthesis, characterization, antimicrobial activity and DNA-binding properties of the mononuclear cobalt(II) complex with the third-generation quinolone sparfloxacin are reported.

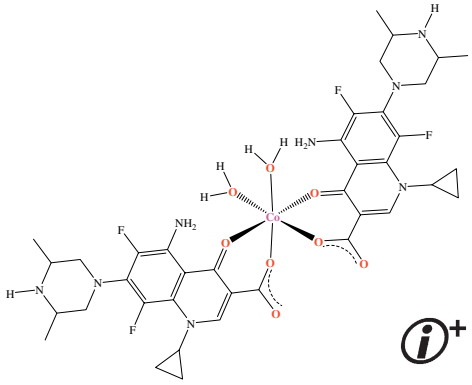



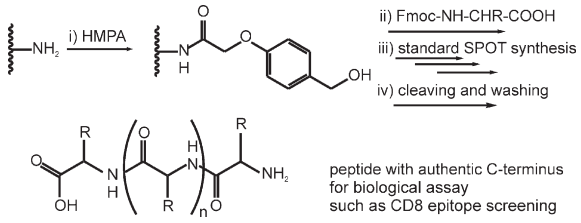


The synthesis of the peptides cleavable peptides with authentic C-termini is reported and validated through T-cell stimulation by a synthesized CMV CD8 T-cell epitope.

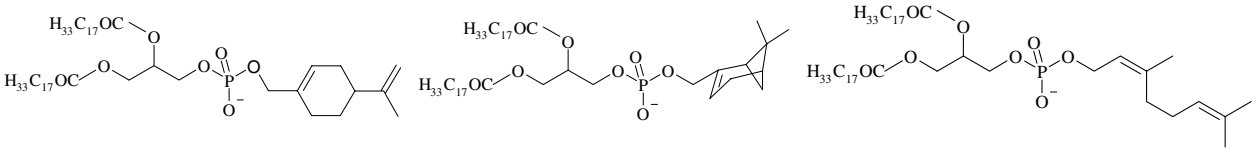

Phosphatidyl-perillyl alcohol (**10**) Phosphatidyl-myrtenol (**12**) Phosphatidyl-nerol (**14**)

Antiproliferative phosphatidylated-monoterpene alcohols were synthesized by phospholipase D catalyzed transphosphatidylation and their effects on human cancer cells were examined.



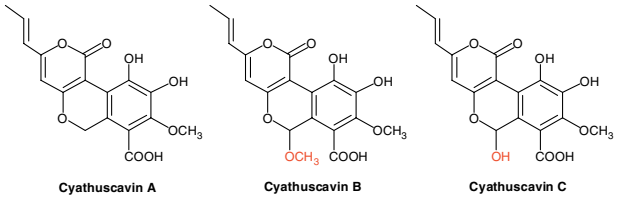


Cyathuscavins A–C (**1**–**3**) showing free radical scavenging activity and DNA protection activity were reported.



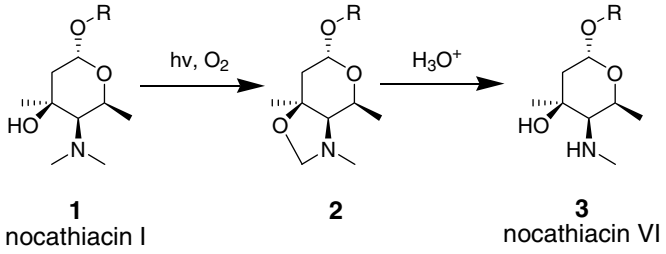


Irradiation of nocathiacin I (**1**) with UV light of 380 nm led to a cyclic product **2**, which was hydrolyzed to yield the desired N-demethylation product, nocathiacin VI (**3**).



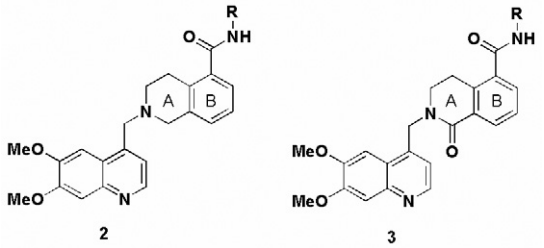


The synthesis, structure–activity relationships and pharmacokinetic properties of 1,2,3,4-tetrahydroisoquinolines (**2**) and 3,4-dihydroisoquinoline-1(2*H*)-ones (**3**), two novel classes of potent KDR inhibitors.

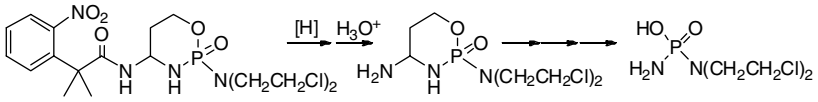


_N_-(2,2-Dimethyl-2-(2-nitrophenyl)acetyl)-4-aminocyclophosphamide isomers were synthesized as potential bioreductively activated prodrugs of phosphoramide mustard and their mechanism of reductive activation was investigated.



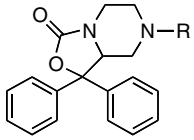


Description: Structural features important for Neuropeptide S antagonist activity have been identified though the synthesis and testing of a series of 7-substituted 1,1-diphenyl-hexahydro-oxazolo[3,4-a]pyrazin-3-ones.



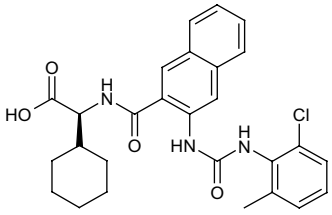


**1c-(S)**: $IC_{50}$ (hLGPa)= 80 nM



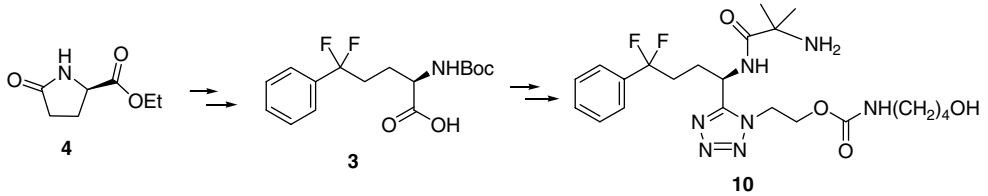


**4** **3** **10**

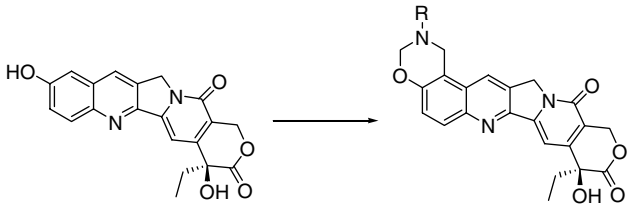

A novel series of A-ring modified hexacyclic camptothecin derivatives containing a 1,3-oxazine ring have been synthesized and evaluated for in vitro cytotoxicity.



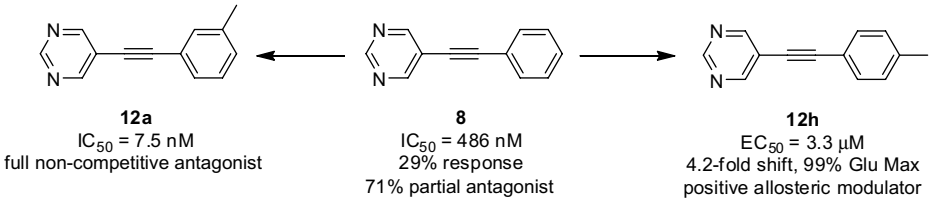


The synthesis and SAR of a mGluR5 allosteric partial antagonist lead **8** is described. We have identified 'molecular switches' on the distal phenyl ring that modulate modes of efficacy from mGluR5 partial antagonism in **8**, to full non-competitive antagonism **12a** to positive allosteric modulation **12h** by the addition of a 3- or 4-methyl group, respectively.



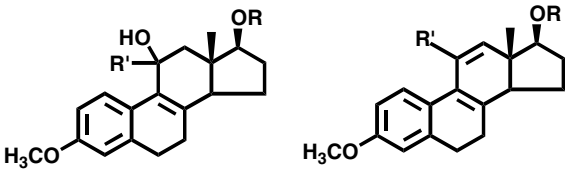

Synthesis of 11-substituted estradiol derivatives (**12**–**17**) has been carried out by the Grignard reaction with alkyl, allyl and benzyl halides on 17β-hydroxy-3-methoxy-11-oxo-estra-1,3,5(10),8(9)-tetraene (**10**). The novel compounds (**10** and **12**–**17**) were evaluated for their preliminary post-coital contraceptive (anti-implantation) activity in Sprague–Dawley rats.



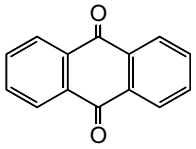

The structure–activity relationships between the inhibitory effects ($\log IC_{50}$) and the first reduction potentials of anthraquinone derivatives are described.

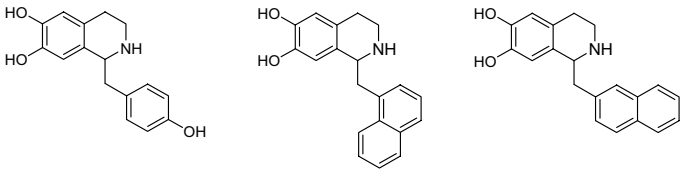


Six optically active tetrahydroisoquinoline alkaloids were synthesized and their effects on platelet anti-aggregation and experimental animal model of the disseminated intravascular coagulation (DIC) and multiple organ failure (MOF) were evaluated.



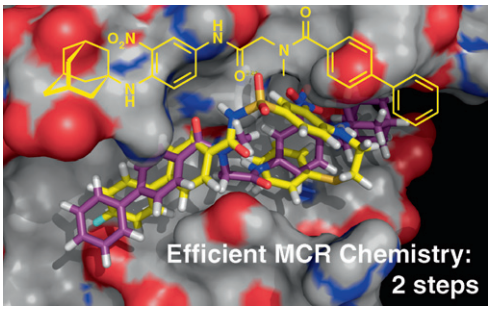




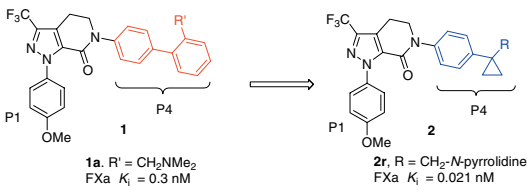


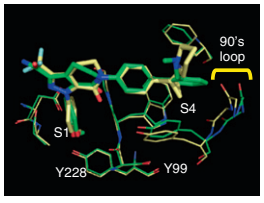


*Ortho*-substituted biphenyl moieties are widely used in drug design. We herein report a successful use of the perpendicular conformation of the alpha-substituted phenylcyclopropyl groups to mimic the aplanar, biologically active conformation of the ortho-substituted biphenyl moieties to achieve structural diversity. This is exemplified by the design and synthesis of a series of highly potent pyrazole bicyclic-based Factor Xa (FXa) inhibitors bearing *alpha*-substituted phenylcyclopropyl P4 moieties. The designed perpendicular conformation was confirmed by the X-ray structure of FXa-bound compound **2r**. The potential structural basis for the high FXa potency in the phenylcyclopropyl P4 analogs and their improved FXa inhibitory activities compared with the biphenyl P4 counterparts are discussed.



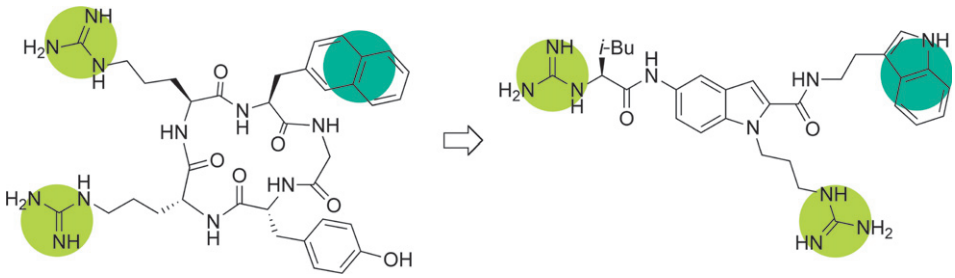

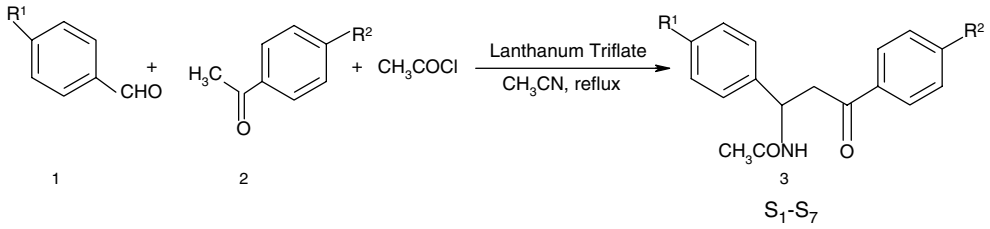




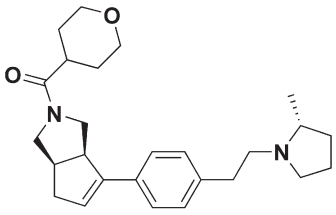


**3u**



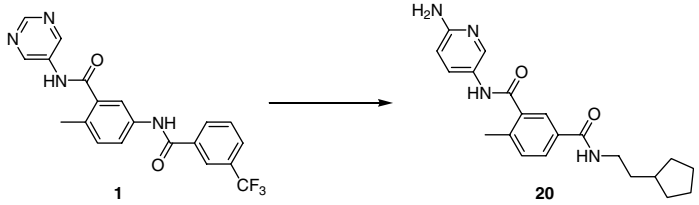


Form the screening of our kinase-preferred library, we have identified **1** as a potent small-molecule c-Kit inhibitor. Extensive structure–activity relationship study, incorporated with modification on PKDM properties have led to a selective c-Kit inhibitor **20**. In an in vivo murine model of mast cell activation, **20** blocked the SCF-induced histamine release with an $EC_{50}$ of 26 nM.



The synthesis and binding studies of a neomycin conjugate capable of binding DNA:RNA hybrids in the sub-nanomolar range is presented.

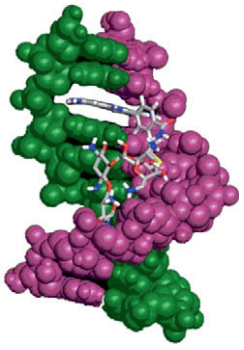

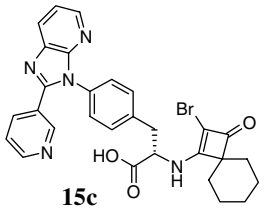


**15c**

The synthesis and SAR of a novel series of imidazopyridine VLA-4 antagonist is described. Compound **15c** is a representative example of this series with a human whole blood $IC_{50}$ of 3 nM.



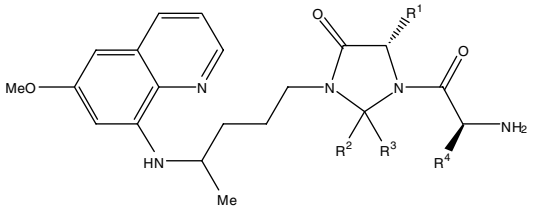


The synthesis and antimalarial activity of imidazolidin-4-one peptidomimetic derivatives of primaquine is reported.



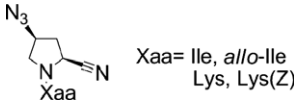




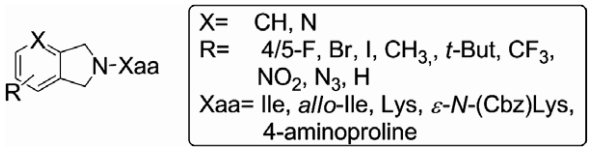

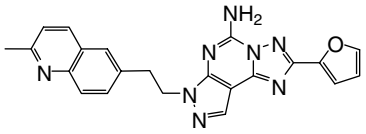

**25**

The design and synthesis of biaryl and heteroaryl analogs of the adenosine $A_{2A}$ receptor antagonist SCH 58261 are reported. Derivatives such as the quinoline **25** improve upon the pharmacological and pharmacokinetic properties of the parent phenethyl compound SCH 58261.



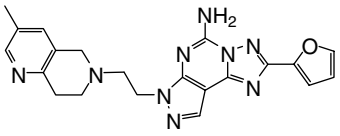

**4s**

The design and synthesis of fused heterocyclic analogs of the adenosine $A_{2A}$ receptor antagonist SCH 58261 are reported. Derivatives such as the tetrahydronaphthyridine **4s** not only improve upon the pharmacological and pharmacokinetic properties of SCH 58261, but also have high aqueous solubility.



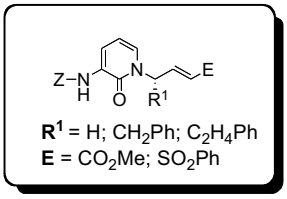


Here we present the design and synthesis of novel peptidomimetic falcipain inhibitors that should react as classical 'Michael acceptors' and in which the incorporation of a rigid scaffold moiety to define a conformation is evaluated for antimalarial activity.



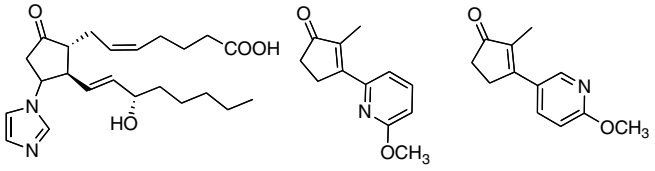


The development of series of small molecule inhibitors of anthrax edema factor is reported.

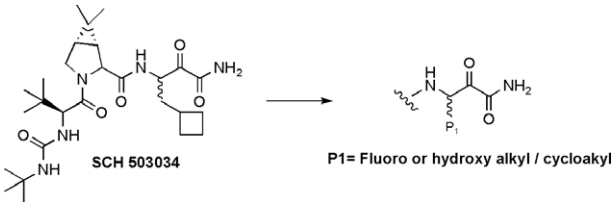




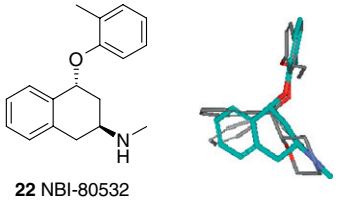


A rigid ring-constrained norepinephrine reuptake inhibitor with potent functional activity at the transporter ($IC_{50}$ = 8 nM) was used to develop a model for the distance and orientation of key features necessary for interaction with NET.



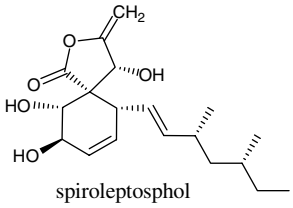




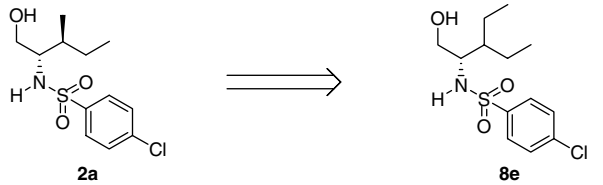


Lead optimization studies of Notch-sparing GSI **2a** led to the discovery of analog **8e** with improved γ-secretase inhibitory potency and Notch-sparing selectivity.

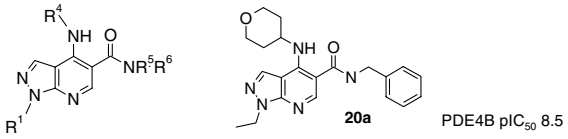


A series of pyrazolo[3,4-*b*]pyridine-5-carboxamides has been identified as potent inhibitors of PDE4. The SAR has been explored and these studies have highlighted compound **20a** which shows good potency, selectivity and rat PK suitable for oral dosing. The crystal structure of **20a** bound to PDE4B is also described.



A series of thiophene carboxamide checkpoint kinase inhibitors (**3**) were discovered through HTS and optimized for cellular potency (**12n**).

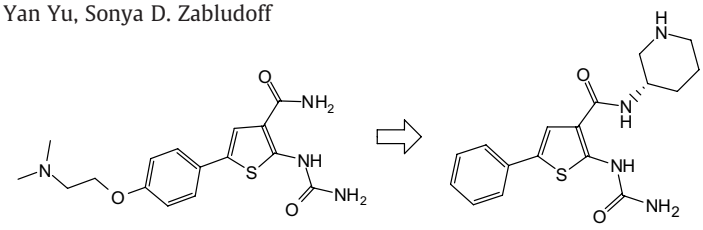




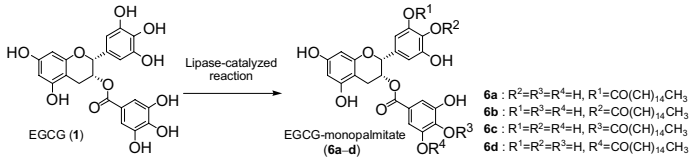


A series of fatty acid monoester derivatives of (−)-epigallocatechin-3-*O*-gallate (EGCG) were prepared by one-pot lipase-catalyzed transesterification. The introduction of long alkyl chains enhanced anti-influenza A/PR8/34 (H1N1) virus activity up to 24-fold relative to native EGCG.

## OTHER CONTENTS



*Corresponding author
ⓘ+ Supplementary data available via ScienceDirect

**COVER**

Overlay of high resolution co-crystal structures of *R*-**22**-ADP (cyan) and **1**-ADP (green) bound in an allosteric binding site of the mitotic kinesin KSP. [Roecker, A. J.; Coleman, P. J.; Mercer, S. P.; Schreier, J. D.; Buser, C. A.; Walsh, E. S.; Hamilton, K.; Lobell, R. B.; Tao, W.; Diehl, R. E.; South, V. J.; Davide, J. P.; Kohl, N. E.; Yan, Y.; Kuo, L. C.; Li, C.; Fernandez-Metzler, C.; Mahan, E. A.; Prueksaritanont, T.; Hartman, G. D. *Bioorg. Med. Chem. Lett.* **2007**, *17*, 5677.]



Indexed/Abstracted in: Beilstein, Biochemistry & Biophysics Citation Index, CANCERLIT, Chemical Abstracts, Chemistry Citation Index, Current Awareness in Biological Sciences/BIOBASE, Current Contents: Life Sciences, EMBASE/Excerpta Medica, MEDLINE, PASCAL, Research Alert, Science Citation Index, SciSearch, TOXFILE

ELSEVIER

ISSN 0960-894X